PHYSICAL REVIEW C VOLUME 18, NUMBER 6 DECEMBER 1978

Uncertainties in neutron densities determined from analysis of 0.8 GeV polarized proton scattering from nuclei

L. Ray
Theoretical Division, Los Alamos Scientific Laboratory, University of California, Los Alamos, New Mexico 87545

W. Rory Coker
Department of Physics, University of Texas, Austin, Texas 78712

G.W. Hoffmann
Department of Physics, University of Texas, Austin, Texas 78712 and Los Alamos Scientific Laboratory, University of California, Los Alamos, New Mexico 87545

(Received 11 July 1978)

The first order, spin-dependent microscopic proton-nucleus optical potential of Kerman, McManus, and Thaler is used to analyze 800 MeV polarized proton elastic differential cross section and analyzing power data for target nuclei ^{58}Ni, ^{90}Zr, ^{116,124}Sn, and ^{208}Pb. Approximately model-independent target neutron density distributions are constructed in order to investigate the uncertainty in the deduced neutron densities resulting from the statistical error and the finite range of momentum transfer in the experimental angular distributions. Numerous other experimental and theoretical sources of error and uncertainty are considered to obtain a realistic estimate of the total error in the deduced neutron densities and their root-mean-square radii. The typical error in the root-mean-square radii is found to be ±0.07 fm. Impressive qualitative agreement is found between the deduced neutron matter densities and the corresponding densities predicted by Hartree-Fock calculations.

[NUCLEAR REACTIONS Proton-nucleus scattering, $E = 0.8$ GeV; targets ^{58}Ni, ^{90}Zr, ^{116,124}Sn, ^{208}Pb; analyzing power; spin-dependent Kerman, McManus, and Thaler optical potential; model-independent densities; error analysis; neutron radii.]

I. INTRODUCTION

The nuclear radius and the shape of the nuclear matter density distribution have received continued study throughout the history of nuclear physics. References 1–21 are some of the more recent works on these topics. A major goal of much of this work has been to obtain empirical matter densities unambiguously enough to permit meaningful comparisons with predictions of the shell model[22] or various self-consistent-field models[23-26] of nuclei.

Experiments with electrons and muons have provided data from which the nuclear charge density has been reliably determined for stable nuclei throughout the table of nuclides.[1-2] Generally, there is good qualitative agreement between the experimental charge densities and those predicted by Hartree-Fock calculations.[1]

Unambiguous neutron density distributions are much harder to obtain. Experimental data from which one can attempt to deduce these densities necessarily involve the hadron-nucleus interaction; thus, scattering experiments with beams of protons, ^{4}He, and pions are used to provide the data for theoretical interpretation. Unfortunately, a model-independent description of the interaction and reaction mechanism is lacking.[13-15,17,27] Also, a correct relativistically invariant equation of motion is not available.[1,27-29] Because of these uncertainties, the neutron distributions deduced using different projectiles and/or different methods of analysis are sometimes found to substantially disagree.[12,15,16] Varma and Zamick offer a brief critique of this situation.[12]

The purpose of this paper is to present a thorough investigation of the sources of uncertainty in the deduced neutron densities found from analysis of 0.8 GeV polarized proton elastic differential cross section and analyzing power data for target nuclei ^{58}Ni, ^{90}Zr, ^{116,124}Sn, and ^{208}Pb. Experimental errors, theoretical models, and assumptions, as well as various systematic errors are considered. This work offers a more detailed explana-

tion and an extension of analyses reported earlier.[5,30-32] The results obtained here, when compared with those from similar "microscopic" optical model analyses of proton-nucleus elastic scattering data at other energies,[8,9,33] and with results of analyses employing multiple scattering theory,[3,4,6,7,10-12] indicate that different analyses of a variety of medium energy proton elastic scattering data give neutron rms radii which agree to within the limits of the stated errors.

The consistency of the results of analyses of medium energy proton-nucleus elastic scattering data is significant and favors the use of medium energy protons as probes of the nuclear density. The advantages appear to be (1) less absorption as compared with elastic pion scattering at energies near the (3, 3) resonance[17,21,34] and with elastic ^{4}He scattering, (2) a better understanding of the scattering process[14,17,27-28] (i.e., lesser importance of higher-order corrections and off-shell effects in the optical potential),[33,35] and (3) lack of internal many-body complications in the projectile (as compared to ^{4}He). The disadvantages are (1) the extra spin degree of freedom of the proton, and (2) a lack of sensitivity, relative to pion scattering, to the distinction between target protons and neutrons.[17-18] The additional complication due to spin-effects can be nullified by the simultaneous analysis of angular distribution and analyzing power or polarization data.[30,32,36-37] As for pion probes being advantageous because they distinguish between target protons and neutrons, an examination of the results of a number of recent surveys of pion-nucleus scattering, indicates that the simultaneous analysis of π^+ and π^- elastic angular distributions does not provide the strong and unambiguous separation of proton-related from neutron-related effects that some had expected on the basis of simple arguments concerning the free pion-nucleon total cross sections. This is most likely due to the neglect in the analyses of important higher-order corrections and off-shell effects in the pion-nucleus optical potential as well as strong absorption.[38,39] The result is a great ambiguity and model dependence in the fits to the angular distributions.

With few exceptions[10] all previous analyses of proton-nucleus scattering at medium energies have made use of specific functional forms for the assumed nuclear densities, and have not included a sufficiently detailed or thorough investigation of the many possible sources of error, both experimental and theoretical, which affect the derived result for the neutron density's root-mean-square radius and overall radial form. In this work, we show how to construct a nuclear density which is approximately model independent[1,40,41] in order to permit a determination of the uncertainty in the deduced neutron density due to the statistical error and finite range of momentum transfer of the experimental data. The error in the deduced neutron density due to numerous other experimental and theoretical uncertainties is also estimated. Only by carefully including all important theoretical and experimental sources of error in the analysis can meaningful comparisons with theoretical predictions of nuclear matter densities or with results of other types of analysis of different kinds of experimental data be made.

In Sec. II, the theoretical model on which the present study is based is discussed, together with details of the mode of the error analysis. In Sec. III, the results obtained from analysis of the available 0.8 GeV proton scattering data are presented and compared to predictions of the density-matrix-expansion variant of Hartree-Fock theory. The results of the error analysis are also presented, in full. In Sec. IV, conclusions are drawn about the usefulness of the medium energy proton as a probe of nuclear structure details. Suggested tests of the microscopic theory of the proton-nucleus optical potential are also given, and, finally, further experimental and theoretical refinements are suggested.

II. THEORY

The optical model analysis presented here was done using the microscopic nucleon-nucleus optical potential formulated by Kerman, McManus, and Thaler (KMT)[27] as modified by Feshbach *et al.*[28] Since the target nuclei to be considered have $A \geq 58$, the potential is calculated only to first order in the nuclear density; various corrections which contribute in second order, such as the center-of-mass and Pauli correlations, as well as possible dynamical correlations, have not been considered explicitly.[33,35] The (small) effect of such corrections on the predicted nucleon-nucleus elastic scattering cross sections will, however, be considered in the study of the total uncertainty in the deduced neutron matter densities of the target nuclei under consideration.

The first order KMT potential, which is referred to as the Rayleigh-Lax or RL potential,[42] is given in terms of the proton-nucleon scattering amplitudes (evaluated in the proton-nucleus center-of-momentum system) and the uncorrelated point densities of the protons and neutrons in the target nucleus. The description of the proton-nucleon scattering in general requires five amplitudes.[43] However, if the target nuclei to be considered all have a ground-state spin of zero, as is the case here, then the average over the target nucleon spin,

which is carried out in generating the RL potential, averages three of the terms to zero. One thus needs to consider

$$t_{pj}(q^2) = t^0_{pj}(q^2) + i t^s_{pj}(q^2)(\vec{\sigma}_p + \vec{\sigma}_j)\cdot\hat{n}\,, \tag{1}$$

where j refers to target protons (p) or neutrons (n), q is the momentum transfer with $\vec{q} = \vec{k}_f - \vec{k}_i$, and $\hat{n} \equiv (\vec{k}_i \times \vec{k}_f)/|\vec{k}_i \times \vec{k}_f|$. For incident nucleon energies near 1 GeV, the spin-independent and spin-dependent parts of $t_{pj}(q^2)$ are conventionally parametrized as[5,44,45]

$$t^0_{pj}(q^2) = (ik_0\sigma^T_{pj}/4\pi)(1 - i\alpha_{pj})\exp(-B_{pj}q^2)\,,$$
$$t^s_{pj}(q^2) = (ik_0\theta_{pj}/4\pi)(q^2/4M^2)^{1/2}(1 - i\alpha_{spj})\exp(-B_{spj}q^2)\,, \tag{2}$$

where M is the nucleon mass. Unfortunately, in order to determine the parameters of Eq. (2) unambiguously, it is necessary to know the complete nucleon-nucleon scattering amplitudes[43] over the range of momentum transfer covered by the proton-nucleus elastic scattering data. The complete set (at least nine) of nucleon-nucleon experiments which provide data from which these amplitudes may be determined have not been done[43,46-47] at energies near 0.8 GeV. The experiments required, such as spin-correlation, double-polarization, and triple-scattering[43] are difficult, and although such experiments are planned at LAMPF and elsewhere, it will be some time before the complete set of data is available. Data presently available[46-49] at energies near 0.8 GeV include pp and pn elastic angular distribution and pp polarization which is insufficient to determine all the parameters of Eq. (2).

However, total cross section[46-47,50] and very-forward-angle scattering data[51-52] do determine $\sigma^T_{pp} = 4.73$ fm^2, $\sigma^T_{pn} = 3.79$ fm^2, and $\alpha_{pp} = 0.056$ (see Table III below for the experimental errors). In the absence of precisely normalized $p+n$ scattering data, dispersion-theory estimates may be consulted, which predict $\alpha_{pn} = -0.3 \pm 0.15$.[53-55] Since assumed values for α_{pj} mainly affect the peak-to-valley ratios of the predicted proton-nucleus elastic angular distributions, and do not shift the patterns in angle or affect the overall slope, the uncertainty in α_{pj} is essentially unreflected in the neutron density one obtains by a fit to the angular distributions. For this reason α_{pn} was allowed to vary to obtain the optimum fit for all nuclei studied so far at 0.8 GeV, including ^{12,13}C, ^{40,48}Ca, ^{54}Fe, ^{58,64}Ni, ^{90}Zr, ^{116,124}Sn, and ^{208}Pb. The resulting value is $\alpha_{pn} = -0.2$.

Recent 0.8 GeV $p+p$ polarization data[56] together with complementary cross section data,[48] as well as data from other sources,[46,47] have allowed verification of the adequacy of the Gaussian forms [Eq. (2)] of the spin-independent and spin-dependent amplitudes out to momentum transfers of 0.5 (GeV/c)^2. From these data one determines that $B_{pp} + B_{spp}$ is roughly 0.3 fm^2, and that $B_{pp} = 0.09$ fm^2 and $B_{spp} = 0.2$ fm^2 give an adequate fit to the $p+p$ elastic cross section and polarization data. In obtaining these values only the two amplitudes in Eq. (1) were assumed. A value of $B_{pn} = 0.12$ fm^2 (taking $B_{spn} = B_{spp}$ in lieu of $p+n$ polarization data[57]) reproduces recent 0.8 GeV $p+n$ cross sections.[46,47,49]

A simultaneous fit to the $p+p$ cross section and polarization data only allows one to determine the quantity $\theta_{pp}(\alpha_{spp} - \alpha_{pp})$ (again neglecting double spin flip amplitudes), so that θ_{pp} is not determined independently of α_{spp}.[43] Only "triple-scattering"-type measurements would allow such a separate determination of the two parameters.[43] If one assumes $\theta_{pp} = \theta_{pn}$ and $\alpha_{spp} = \alpha_{spn}$ and chooses these parameters to fit the $p+p$ polarization data at 0.8 GeV, or alternatively uses values interpolated from those suggested for other energies by Auger, *et al.*,[45] it is found that the predicted proton-nucleus analyzing power overestimates the overall strength of the data.[30,32] Because the θ_{pj} and α_{spj} appear in the RL potential in isospin-weighted sums, the approach adopted here was to define isospin-averaged quantities $\bar{\theta}_p$ and $\bar{\alpha}_{sp}$ (along with $\bar{B}_{sp}$) and adjust $\bar{\theta}_p$ and $\bar{\alpha}_{sp}$ to fit the proton-*nucleus* analyzing power data. Since there is no reason to expect the $p+p$ and $p+n$ spin parameters to be the same, one anticipates that the isospin-averaged parameters should vary smoothly with the ratio N/Z of the particular nucleus.[31,32] There is no alternative at present to the semiphenomenological treatment of spin-effects adopted here; better and more complete experimental determination of the various nucleon-nucleon amplitudes is necessary before the proton-nucleus phenomenology can give way to nucleon-nucleon phenomenology.

We begin by considering a conventional model-dependent analysis, by assuming a specific form for the point-nucleon matter densities of the target nucleus, namely,[31]

$$\rho_j(r) = \rho_{0j}\big((1 + w_j r^2/R_j^2)/\{1 + \exp[(r^k - R_j^k)/z_j^k]\} + s_j\cos(m_j r - \phi_j)\exp[-d_j(r - r_{0j})^2] + s'_j\exp[-d'_j(r - r'_{0j})^2]\big)\,, \tag{3}$$

where $k = 1$ or 2, $j = p$ or n, and ρ_{0j} is adjusted to insure normalization to the proper number of target nucleons. The second and third terms are used only for the point-proton density of ^{208}Pb, these being necessary in order to reproduce the sum-of-Gaussians (SOG) charge density[40] obtained from recent electron scattering data[58] which extend to large momentum transfer (3.7 fm^{-1}).

Once the RL potential is constructed, it is inserted into the Schrödinger equation,[59]

$$[d^2/dr^2 - l(l+1)/r^2 - 2\mu U_{jl}^{\mathrm{RL}}(r)/\hbar^2 + k_N^2]\chi_{jl}(r) = 0\,, \tag{4}$$

where k_N is the exact relativistic wave number in the center-of-momentum (c.m.) system and μ is the "reduced energy"[59] in amu (i.e., $\mu = \epsilon_1\epsilon_2/(\epsilon_1 + \epsilon_2)$, where ϵ_i is the total relativistic c.m. energy of particle i in amu). The representation of the spin-dependent RL potential in coordinate space is denoted by $U_{jl}^{\mathrm{RL}}(r)$,[33,44] and includes a Coulomb interaction constructed via a folding model from the nuclear charge density as determined from electron scattering.[2,58]

The procedure followed for the conventional calculation is outlined below. First, the point-proton densities, in the form of Eq. (3), were determined by unfolding the single proton charge form factor from the empirical nuclear charge form factors determined from electron scattering experiments. The small effect of the neutron charge form factor has been neglected.[60] The resulting proton matter densities were then kept fixed. For the neutron densities only the first term of Eq. (3) was considered. The parameters w_n, R_n, and z_n, as well as $\bar{\theta}_p$ and $\bar{\alpha}_{sp}$, were freely searched for each nucleus to simultaneously fit the differential cross section and analyzing power data according to the $|\chi|^2$ criterion.

Because of the above procedure, the derived "neutron densities" (1) necessarily reflect the uncertainties associated with the nucleon-nucleon amplitudes and the omission of higher-order terms in the optical potential, (2) are model-dependent, and (3) are dependent on systematic errors in the data. Hence, the derived neutron densities are referred to as the Rayleigh-Lax (RL) densities to distinguish them from the true neutron densities.

At this point an investigation needs to be made of the ways in which the various above-mentioned uncertainties, as well as those inherent in the theoretical approach itself,[27,28] are reflected in the derived RL neutron densities. For the analysis of electron scattering data, a number of techniques exist in the literature for evaluating the uncertainty in the charge density. Friar and Negele[1,41] have shown that a linear Fourier-Bessel series expansion of the density leads to the full error matrix[1] which is expressed directly in terms of the chosen basis functions, the experimental error, and a kernel which relates the density to the observed lepton-nucleus scattering amplitude. Extension of this approach to hadron-nucleus scattering is not satisfactory because the kernel depends strongly on the dynamics of the hadron-nucleus interaction, and therefore, is dependent of the specific model chosen for the description of the interaction.[27,28]

Another popular method for "model-independent" analysis of electron scattering data is that introduced by Sick.[40] In this approach the charge density is represented by a sum of Gaussians (SOG), and Monte-Carlo techniques are used to choose the positions of the Gaussians at random. The strengths of the Gaussians are adjusted to optimize the $|\chi|^2$ of the fit. All densities which lead to fits which have $|\chi|^2$ below some arbitrary minimum are then superimposed to provide an error envelope which indicates how well the detailed radial shape of the charge density is determined. Limited application of this method in the analysis of proton and ^{4}He elastic data has previously been made.[10,13]

The approach taken here for generating error envelopes for the neutron densities is distinct from the two techniques mentioned above, although it does use a Monte-Carlo technique which is analogous to that of the Sick approach.[40] The RL neutron density is generalized to

$$\rho_n(r) = b[\rho_n^0(r) + S\Delta\rho_n(r)]\,, \tag{5}$$

where $\rho_n^0(r)$ is taken to have the form of Eq. (3). Perturbations to this density, $\Delta\rho_n(r)$, are chosen at random, as more fully discussed below, and the strength S of each perturbation is increased until the fit to the experimental data deteriorates. The constant b is re-evaluated for each perturbation to insure the proper overall normalization of $\rho_n(r)$. With a sufficient number of randomly chosen $\Delta\rho_n(r)$ an error envelope for $\rho_n(r)$ emerges.

Two forms for the perturbations $\Delta\rho_n(r)$ are used here, a sum of Gaussians (SOG)[40] and a sum of Bessel functions (SOBF)[41]:

$$\Delta\rho_n(r) = (2\pi^{3/2}\gamma^3)^{-1}\sum_{i=1}^{w} Q_i(1 + 2c_i^2/\gamma^2)^{-1}\{\exp[-(r-c_i)^2/\gamma^2] + \exp[-(r+c_i)^2/\gamma^2]\} \tag{6}$$

and

$$\Delta\rho_n(r) = \begin{cases} \sum_{\nu=1}^{M} a_\nu j_0(\pi\nu r/R)\,, & r \le R \\ 0\,, & r > R\,. \end{cases} \tag{7}$$

For the SOG perturbations, w is taken to be 12 or less.[10,13,40,58] The relative strengths Q_i and the positions c_i are randomly distributed over the ranges 0 to 1 and 0 to gR_n, respectively, where R_n is the parameter appearing in Eq. (3) and g varies from about $\frac{1}{2}$ to 2. Since Hartree-Fock calculations predict structure in the nuclear matter densities due to oscillations of the Hartree-Fock state functions of the individual nucleons, one may impose the condition that oscillations allowed in the density, Eq. (6), be no smaller in radial extent than those predicted by Hartree-Fock.[23-26] This leads to the condition that $\gamma \approx 1.2$ to 1.4 fm.[10,13,40,58] For the present calculations γ was fixed to a value of 1.39 fm,[58] and it was required that the constants Q_i be positive.[40]

When the SOBF form is used for $\Delta\rho_n(r)$, the a_ν are randomly distributed between -1 and 1, the number of terms M is $2R/\lambda_{\min}$ ($\lambda_{\min}$ is the smallest oscillation allowed in the density and is taken to be 1.5 fm),[23-26,41] and the range R is given as before by gR_n. For both the SOG and SOBF approaches, $\rho_n(r)$ is not allowed to be negative.

The procedure for finding an acceptable density, given a set of randomly chosen Q_i and c_i (or a_ν), is described as follows. Starting with the best fit given by $\rho_n^0(r)$ ($b=1$, $S=0$) the quantity

$$\left|d\sigma(\text{theory},\ S=0)/d\Omega_k - d\sigma(\text{exp})/d\Omega_k\right|$$

is evaluated at each data point k. Only the angular distribution data is considered since the analyzing power data do not impose nearly as severe a limitation on $\rho_n(r)$ at present. The importance of the analyzing power data is that it allows the effective spin-dependent terms in the nucleon-nucleon amplitudes to be determined (see Sec. III B). The strength of the scale factor S [Eq. (5)] is then increased until

$$\left|d\sigma(\text{theory},\ S\neq 0)/d\Omega_k - d\sigma(\text{exp})/d\Omega_k\right| - \left|d\sigma(\text{theory},\ S=0)/d\Omega_k - d\sigma(\text{exp})/d\Omega_k\right| = \Delta\sigma_{\text{exp},k}\,, \tag{8}$$

for any data point k, where $\Delta\sigma_{\text{exp},k}$ is the experimental statistical error associated with that point.

Long range variations in the model density $\rho_n^0(r)$ were treated by varying the parameters w_n, R_n, and z_n of Eq. (3) about their optimized values until a relationship analogous to Eq. (8) was satisfied. No $\Delta\rho_n(r)$ terms were included in these calculations.

The approach described in the preceding paragraphs has a number of advantages. The uncertainty in the extracted neutron density due to the experimental error of the data, and the finite range of momentum transfer covered,[1] is evaluated. Information is obtained about how well the neutron density can be determined in principle from the data, and also about how well the original model-dependent analysis which provided $\rho_n^0(r)$ did determine it, since the variation allowed in S depends strongly on the goodness of fit to the data provided by the original choice for $\rho_n^0(r)$. A further advantage is numerical since it is faster to search on the single parameter S, which carries one further and further away from the original density choice, than to search simultaneously on a dozen or so Gaussian strengths Q_i for each set of randomly selected Gaussian positions.[10,40]

In the next section the results of the model-dependent and model-independent analyses are discussed.

III. RESULTS OF THE ANALYSIS

A. Model-dependent analysis and comparison with other results

The results of the initial model-dependent analyses of proton elastic scattering angular distribution and analyzing power data at 0.8 GeV for targets ^{58}Ni, ^{90}Zr, ^{116,124}Sn, and ^{208}Pb have been presented elsewhere.[5,31-32] Table I gives the point-nucleon density parameters for protons and neutrons, and the two searched nucleon-nucleon parameters $\bar{\theta}_p$ and $\bar{\alpha}_{sp}$ for each of the five nuclei considered. Also given are the root-mean-square (rms) radii of the point-proton, point-neutron, and charge densities. For the point-proton density of ^{208}Pb all terms in Eq. (3) were required, as mentioned in Sec. II, to reproduce the model-independent charge density of Frois *et al.*[58] The values used for the second and third terms of Eq. (3) for this case are given by Ray *et al.*[31]

Figures 1 and 2 show the quality of fits to the elastic differential cross sections and analyzing powers obtained from the model-dependent analysis using the parameters of Table I. As seen in Fig. 1 the fits employing the RL potential are excellent, except for the slight back-angle discrepancy seen for ^{208}Pb.

An attempt was made to improve the fit to the ^{208}Pb data by including the second and third terms of Eq. (3) in the neutron density. The technique used to evaluate these terms is similar to one that has been used in analyses of electron scattering data.[61-62] The quantity

$$\tilde{\rho}_{(1)}(q^2) = \tilde{\rho}_{(0)}(q^2)\left\{\left[d\sigma_{\text{exp}}(q^2)/d\Omega\right]/\left[d\sigma_{\text{theo}}(q^2)/d\Omega\right]\right\}^{1/2}, \tag{9}$$

was evaluated, where $\tilde{\rho}_{(0)}(q^2)$ is the Fourier transform of the neutron density given by the first term of Eq. (3) and Table I, and $d\sigma_{\text{theo}}(q^2)/d\Omega$ is the cross section predicted by this density. A correc-

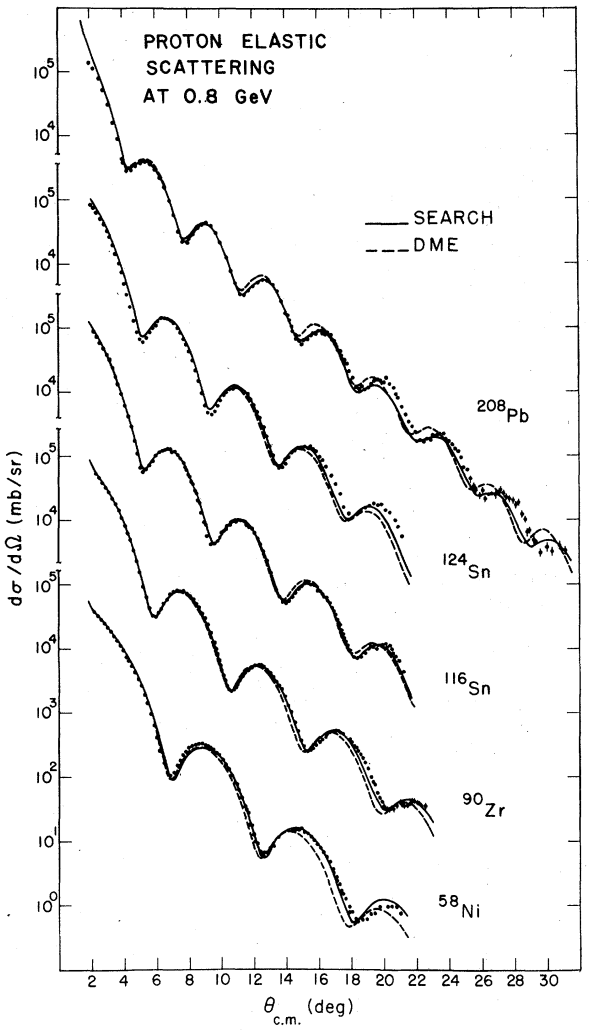

FIG. 1. Proton elastic scattering at 0.8 GeV on targets ^{58}Ni, ^{90}Zr, ^{116,124}Sn, and ^{208}Pb. The solid curves are obtained using the RL optical potential, with the proton densities fixed via electron scattering, while the neutron densities are varied to optimize the fit. The dashed curves result from use in the calculations of point neutron and proton densities predicted by the DME Hartree-Fock. (See Ref. 26 of Negele.) Errors in the data are smaller than the data points when not explicitly indicated.

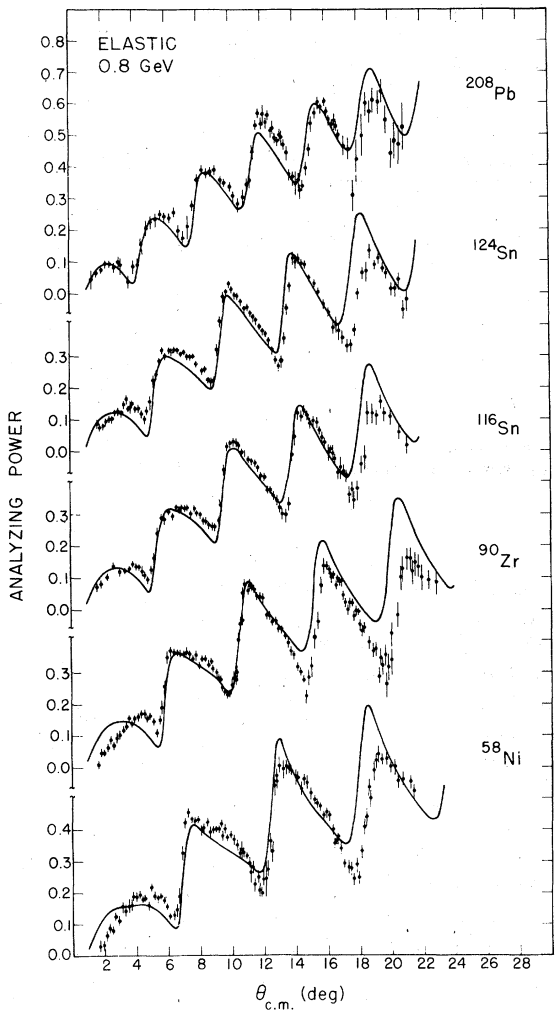

FIG. 2. Proton elastic analyzing power data and predictions at 0.8 GeV for ^{58}Ni, ^{90}Zr, ^{116,124}Sn, and ^{208}Pb. The curves result from use of the RL potential, freely searched neutron densities, and the spin-dependent parameters of Table I.

tion to the original density was then obtained in the form $\Delta\rho_n(r) = \rho_{(1)}(r) - \rho_{(0)}(r)$ where $\rho_{(1)}(r)$ is the inverse transform of $\tilde{\rho}_{(1)}(q^2)$ of Eq. (9). This correction was then fit by the second and third terms of Eq. (3). Since the Born approximation is only roughly valid at these energies, Eq. (9) only provides starting values for the parameters of the second and third terms of Eq. (3). These parameters were then varied to optimize the final fit. Even with this additional flexibility in the form of the RL potential, the back-angle data for ^{208}Pb could not be fit well without sacrificing the agreement at forward angles.

However, Harrington and Varma[35] have shown that Pauli correlations become important at large momentum transfer for heavy nuclei. Results of their calculations indicate that, when treated properly, Pauli correlations cause at back angles both a decrease in slope and an outward shift in angle of the predicted diffractive angular distributions. (See note added in proof.) A recent calculation by Varma and Zamick[12] which includes Pauli correlations provides an excellent fit to the 0.8 and 1.0 GeV ^{208}Pb data at all angles. Their result for the neutron rms radius

TABLE I. The results of the model-dependent analysis discussed in the text. The first four columns give the numerical values of the parameters of Eq. (3) in the text. The root-mean-square (rms) radii for the point-nucleon density distributions are listed in the column under $\langle r^2\rangle^{1/2}$. The quantity $\langle r^2\rangle_{ch}^{1/2}$ is the rms radius of the charge form factor taken from electron scattering; Ref. 58 for ^{208}Pb and Ref. 2 for all others. The last three columns give the numerical values of the spin-dependent parameters, Eq. (2).

Nucleus		w	R (fm)	z (fm)	k	$\langle r^2\rangle^{1/2}$ (fm)	$\langle r^2\rangle_{ch}^{1/2}$ (fm)	$\bar{\theta}_p$ (fm^2)	$\bar{\alpha}_{sp}$	$\bar{B}_{sp}$ (fm^2)
^{58}Ni	p	−0.13	4.30	0.47	1	3.688	3.774	11.8	0.50	0.2
	n	−0.02	4.07	0.50	1	3.652	···	11.8	0.50	0.2
^{90}Zr	p	0.32	4.55	2.41	2	4.204	4.280	11.2	0.55	0.2
	n	0.56	4.49	2.45	2	4.289	···	11.2	0.55	0.2
^{116}Sn	p	0.23	5.14	2.50	2	4.549	4.619	10.4	0.58	0.2
	n	0.32	5.02	2.70	2	4.679	···	10.4	0.58	0.2
^{124}Sn	p	0.26	5.22	2.49	2	4.602	4.671	10.0	0.56	0.2
	n	0.42	5.29	2.67	2	4.823	···	10.0	0.56	0.2
^{208}Pb	p[a]	0.36	6.45	2.65	2	5.443	5.502	9.0	0.63	0.2
	n	0.36	6.19	3.13	2	5.625	···	9.0	0.63	0.2

[a] Additional correction terms included, see Ref. 31 and Eq. (3).

agrees to within 0.03 fm of the value determined in this analysis.

In Fig. 2 it is seen that, in general, the theoretical analyzing power differs from the data sometimes near the first and always near the final maximum. The lack of agreement at forward angles may be due to experimental difficulties[30] since it is not observed for targets such as ^{40,48}Ca, ^{54}Fe, ^{64}Ni, and ^{208}Pb. The discrepancy at back angles is most likely genuine, and is seen for all nuclei studied so far. The forms chosen for the amplitudes of Eq. (1) [given in Eq. (2)] were verified to be valid out to the largest momentum transfer covered by the data. Numerous calculations were

TABLE II. Comparison of proton scattering analyses and Hartree-Fock predictions for $\langle r_n^2\rangle^{1/2}$, $\Delta r_{np} = \langle r_n^2\rangle^{1/2} - \langle r_p^2\rangle^{1/2}$. All radii are in fermis.

Method		Nucleus ^{58}Ni	^{90}Zr	^{116}Sn	^{124}Sn	^{208}Pb
This	$\langle r_p^2\rangle^{1/2}$	3.688	4.204	4.549	4.602	5.443
analysis[a]	$\langle r_n^2\rangle^{1/2}$	3.652	4.289	4.679	4.823	5.625
	Δr_{np}	−0.036	0.085	0.13	0.22	0.18
Δr_{np} from	Ref. 3[b]	−0.043	···	···	···	···
other (p,p)	Ref. 6	···	···	···	···	0.26
analyses	Ref. 8[b]	−0.07	···	···	···	···
	Ref. 9	···	···	···	···	0.25
	Ref. 11[b]	···	0.07	···	···	0.04 (1.0 GeV)
	Ref. 12[b]	···	···	···	···	0.21 (1.05 GeV) 0.21 (0.8 GeV)
DME[c]	$\langle r_p^2\rangle^{1/2}$	3.765	4.243	4.582	4.627	5.461
	$\langle r_n^2\rangle^{1/2}$	3.766	4.322	4.703	4.835	5.660
	Δr_{np}	0.001	0.079	0.121	0.208	0.199
Other	$\langle r_p^2\rangle^{1/2}$	···	4.14–4.24	···	···	5.37–5.465
Hartree-	$\langle r_n^2\rangle^{1/2}$	···	4.19–4.32	···	···	5.49–5.68
Fock[d]	Δr_{np}	···	0.05–0.12	···	···	0.11–0.23

[a] Typical errors for $\langle r_n^2\rangle^{1/2}$ and Δr_{np} are ±0.07 fm (see Table III).
[b] Typical errors are quoted as 0.05 fm.
[c] Using Negele's DME code, Ref. 26.
[d] Range of values includes those given in Refs. 23–26.

made in which the values of all three spin-dependent parameters of Eq. (2) were varied; no substantial improvement in the fits to the last peaks in the analyzing power data resulted. It is known[33,35] that Pauli correlations do not significantly affect the angular distributions until the momentum transfer is about 3.5 fm^{-1}. However, this conclusion may not be valid for the analyzing power (which extends to a momentum transfer of about 2.5 fm^{-1}).

Numerous self-consistent models of the nucleus exist with which the empirical results obtained here may be compared. Shown in Fig. 1 as dashed curves are predictions for the angular distributions obtained using the same spin-dependent amplitudes used to generate the solid curves, but with point-proton and point-neutron densities taken from the density-matrix-expansion (DME)[26] approach to Hartree-Fock theory.[23] These predictions are rather satisfactory, especially for ^{90}Zr and ^{116}Sn, although the total matter radius appears somewhat too large in general. However, inclusion of Pauli correlations into the calculations would slightly decrease the overall slope of the predicted diffractive pattern,[33,35] resulting in improved agreement with the data for several cases. It is worthwhile to note that theoretical uncertainties in matter radii resulting from use of alternate formulations of Hartree-Fock theory (such as the DME or density-dependent Hartree-Fock) and different effective nucleon-nucleon interactions[23-26] are sufficient to encompass the experimental values obtained here[5,31,32] for the majority of cases.

Table II compares the neutron rms radii obtained from the present analysis and other analyses[3,6,8,9,11,12] of medium energy proton elastic scattering data with the DME and other published Hartree-Fock predictions.[23-26]

B. Empirical determination of the spin-dependent amplitudes

As explained in Sec. II one expects an N/Z dependence of the isospin-averaged nucleon-nucleon spin parameters $\bar{\theta}_p$ and $\bar{\alpha}_{sp}$ which are obtained empirically from fitting the analyzing powers (see Fig. 2). The proton-nucleon elastic polarization is insensitive to the value chosen for α_{spj}. However, the proton-nucleus analyzing power is sensitive to $\bar{\alpha}_{sp}$ since it determines peak-to-valley ratios. With this sensitivity the independent uncertainties in the deduced values of $\bar{\theta}_p$ and $\bar{\alpha}_{sp}$ are ±20%. Using the results given in Table I and the results of other analyses,[63] one obtains the explicit N/Z dependence of the two parameters: $\bar{\theta}_p = [23.6 - 9.2(N/Z) \pm 2]$ fm^2 and $\bar{\alpha}_{sp} = 0.17 + 0.28(N/Z) \pm 0.1$. The quoted errors include the uncertainty in $\bar{B}_{sp}$ (which can be varied from 0.1 to 0.3 fm^2) and effects due to the model dependence of the nuclear densities [estimated by repeating the $k=1$ analysis with $k=2$, or vice versa: see Eq. (3)].

In proton-nucleon polarization analyses, the product $\theta_{pj}(\alpha_{spj} - \alpha_{pj})$ can be well determined provided one neglects double spin flip amplitudes. The same is true for proton-nucleus analyzing power analyses in that the product $\bar{\theta}_p \alpha_{sp}$ is better determined than either of the two parameters separately, the uncertainty in the product being about ±10%. Empirically this product varies from about 6.4 fm^2 for $N/Z=1$ to about 5.7 fm^2 for $N/Z=1.5$, indicating that at 0.8 GeV $\theta_{pn}(\alpha_{spn} - \alpha_{pn})$ should be smaller than $\theta_{pp}(\alpha_{spp} - \alpha_{pp})$.[46,49,57]

The necessity at present of determining $\bar{\theta}_p$ and $\bar{\alpha}_{sp}$ from the proton-nucleus analyzing power data itself is illustrated in Fig. 3, for the case of $\vec{p} + ^{116}Sn$. The solid curve is the result of a free search on $\bar{\theta}_p$ and $\bar{\alpha}_{sp}$ with $\bar{B}_{sp}$ fixed at 0.2 fm^2, which gives $F \equiv \bar{\theta}_p(\bar{\alpha}_{sp} - \bar{\alpha}_p) = 6.9$ fm^2, where $\bar{\alpha}_p = (Z/A)\alpha_{pp} + (N/A)\alpha_{pn}$. The dashed curve shows the result using spin-dependent proton-nucleon parameters interpolated from the tabulation of Auger *et al.*,[45] giving $F = 9.0$ fm^2. The dash-dot curve shows the result of using parameters obtained by fitting proton-proton cross section and polarization data at 0.8 GeV,[56] giving $F = 14.4$ fm^2. Clearly, as mentioned in Sec. II, one must for now make use of the freely searched parameters.

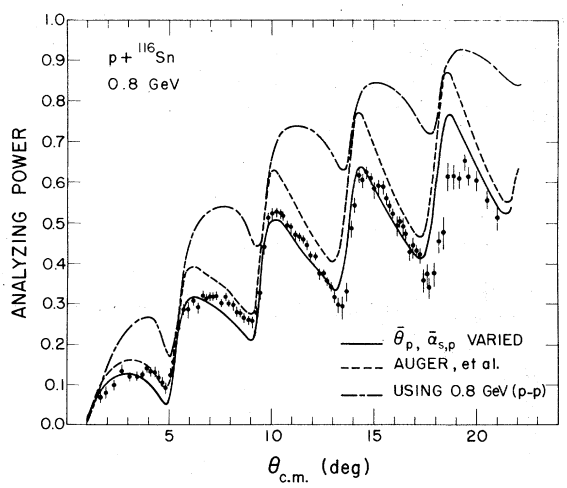

FIG. 3. Predicted elastic analyzing power for $p + ^{116}Sn$ at 0.8 GeV using: (1) empirical spin-dependent parameters (Table I) (solid curve); (2) the spin amplitudes suggested by Auger *et al.* (Ref. 45 and dashed curve); and, (3) proton and neutron spin-dependent amplitudes both fixed to values obtained from $p+p$ polarization data at 0.8 GeV (Ref. 56 and dashed-dot curve).

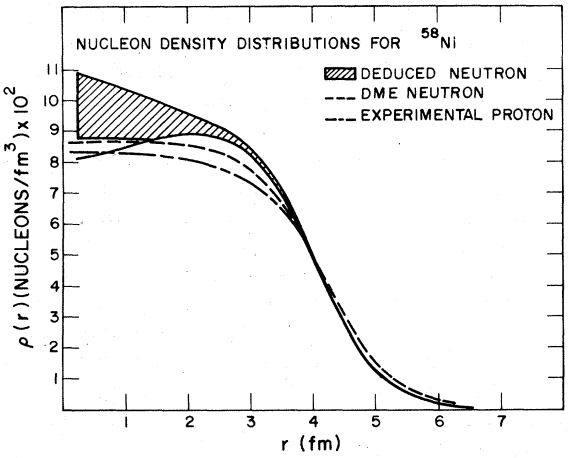

FIG. 4. Point nucleon densities for ^{58}Ni. The shaded band is the error envelope encompassing all the trial SOG neutron densities deduced with the RL potential as explained in the text. Only statistical errors in the data, and model dependence are allowed to contribute to this error band. Shown also is the DME point neutron density (dashed curve) and the point proton density inferred from electron scattering results (no error band given). Note that the DME neutron density is slightly larger than the deduced neutron density envelope in radial extent.

C. Uncertainty in $\rho_n^{RL}(r)$ due to statistical error and finite momentum transfer

The specific procedure adopted for determining the error envelope for the derived neutron densities due to statistical error and finite momentum transfer of the data is discussed below. Using the SOG form [Eq. (6)], 40 randomly generated point neutron densities were found for each nucleus by application of Eq. (8). Six additional densities for each nucleus were also obtained by varying the parameters of Eq. (3) as discussed in Sec. II. Superposition of the 46 densities for each nucleus then defined error envelopes with widths that changed rapidly and characteristically with r.[10,40-41] The error envelopes for the point neutron densities are shown in Figs. 4–8.

The stability of the error envelopes was then investigated by generating 25 additional densities for each nucleus. For all cases the envelopes did not change significantly. To investigate the dependence of the above results on the form chosen for the random densities, the SOBF form [Eq. (7)] was used to generate 30 densities for each nucleus. The error envelopes found here were the same for $r>1$ fm as those found using the SOG technique.

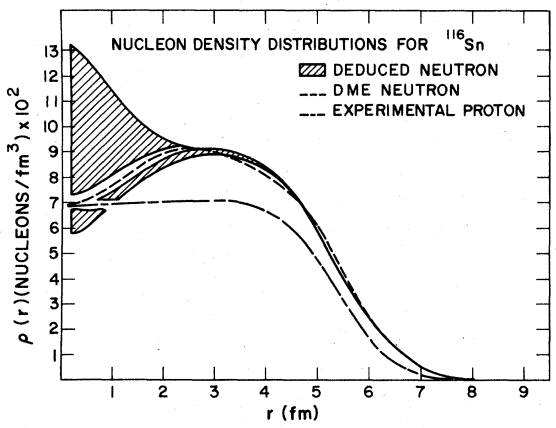

FIG. 6. Same as Fig. 4, except for ^{116}Sn. Generally good agreement between DME and the deduced neutron density is again obtained.

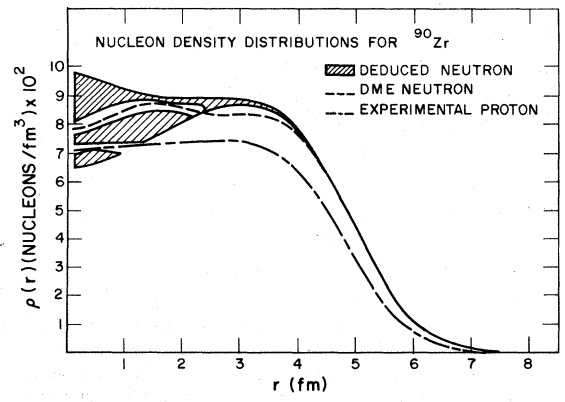

FIG. 5. Same as Fig. 4, except for ^{90}Zr. Note the excellent agreement between DME and the deduced neutron densities in the surface region.

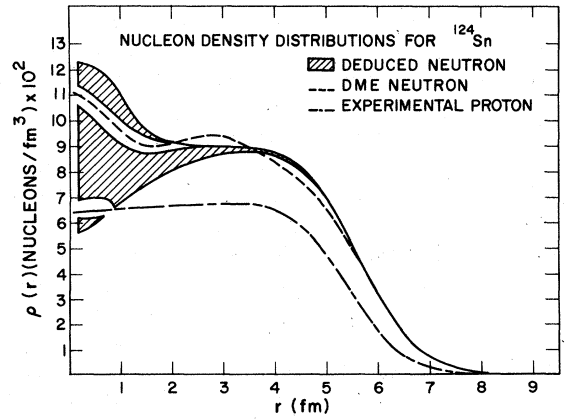

FIG. 7. Same as Fig. 4, except for ^{124}Sn. Notice that the DME neutron density has a greater diffuseness than what is inferred from the proton-nucleus data.

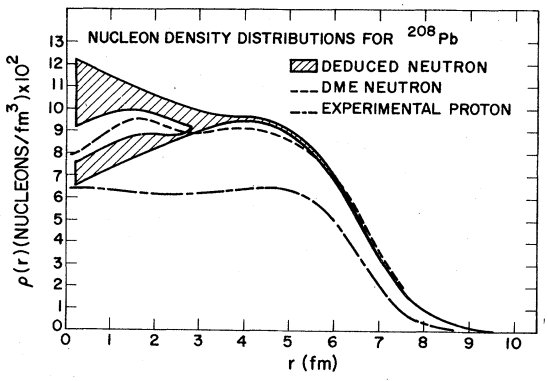

FIG. 8. Same as Fig. 4, except for ^{208}Pb. Note again the larger diffuseness of the DME neutron density as compared with the envelope of deduced RL neutron densities.

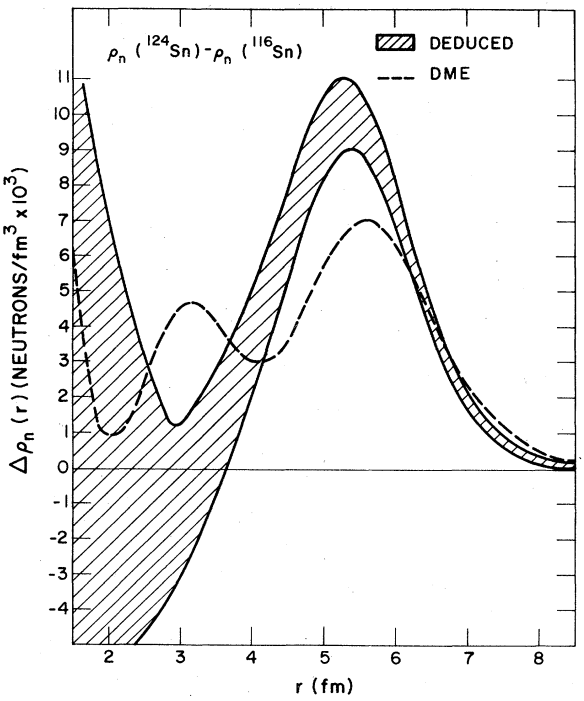

FIG. 9. Shown is the difference between the deduced point neutron densities of ^{124}Sn and ^{116}Sn. The shaded band is obtained from the error envelopes in Figs. 6 and 7. The dashed curve is the DME result. Qualitative agreement is obtained, particularly beyond 4 fm.

For $r<1$ fm the SOBF envelopes were somewhat wider than the SOG envelopes. Thus, except near the origin, the results obtained are essentially independent of the form used for $\Delta\rho_n(r)$ to generate the random densities.

The dashed curves of Figs. 4–8 are point-neutron densities predicted using the DME code of Ref. 26. No attempt was made to determine a "theoretical" error band, since the intent is simply to indicate qualitatively the nature of typical Hartree-Fock calculations. Also shown in Figs. 4–8, as dot-dash curves, are the point-proton densities obtained from analyses[2,58] of electron scattering data. The empirical differences between the proton and neutron matter densities for the nuclei considered is apparent.

Overall there is impressive agreement between the DME predictions for the neutron densities and the empirical densities found here from optical model analysis using the RL potential. Including Pauli correlations would result in a slightly greater diffuseness for the deduced neutron densities and should generally improve the agreement with the DME predictions. It is interesting to compare the theoretical and empirical neutron density differences for the ^{116,124}Sn isotopes, since it can be argued that empirical density differences should be more accurately determined than the densities themselves because of cancellations of uncertainties in the method of analysis. The shaded region of Fig. 9 is the ^{124}Sn-^{116}Sn empirical density difference obtained here, while the dashed curve is the DME prediction for this difference. The agreement is remarkably good.

For each nucleus the mean, $\bar{\rho}_n(r)$, and standard deviation, $\Delta\rho_{n,\mathrm{st}}(r)$, of the random densities were computed at each radial mesh point r. Typically, $[\Delta\rho_{n,\mathrm{st}}(r)/\bar{\rho}_n(r)]\times 100\%$ is 7–15% at $r=0$, 0.6% at the position where $\bar{\rho}_n(r)=0.9\bar{\rho}_n(0)$, 0.8% at $0.5\bar{\rho}_n(0)$, 1.0% at $0.1\bar{\rho}_n(0)$, and rises to 100% at $r \approx 2.2\langle r_n^2\rangle^{1/2}$. For ^{116}Sn, this quantity is shown in Fig. 10 as the dashed curve. Also shown as the solid curve is $[(\rho_{n,\max}(r)-\rho_{n,\min}(r))/(2\bar{\rho}_n(r))]\times 100\%$, where $\rho_{n,\max}(r)$ and $\rho_{n,\min}(r)$ are the upper and lower bounds of the error envelope of Fig. 6. The three arrows in Fig. 10, labeled 90%, 50%, and 10% indicate the radii at which $\bar{\rho}_n(r)$ is 90%, 50%, and 10% of $\bar{\rho}_n(0)$. Figures 4–10 indicate that the nuclear surface is the region most accurately probed by analysis of proton-nucleus elastic scattering data at 0.8 GeV. The insensitivity to the region beyond the surface follows from the density being vanishingly small there.

Only a few percent of the widths of the error envelopes originate from the finite range of momentum transfer covered by the data.[58] For this reason, the envelope widths are almost entirely determined by the statistical errors of the data. Smaller statistical and systematic errors, rather than data of the present statistical quality extending to higher momentum transfer, would be appropriate for reducing the uncertainties in $\rho_n^{\mathrm{RL}}(r)$.

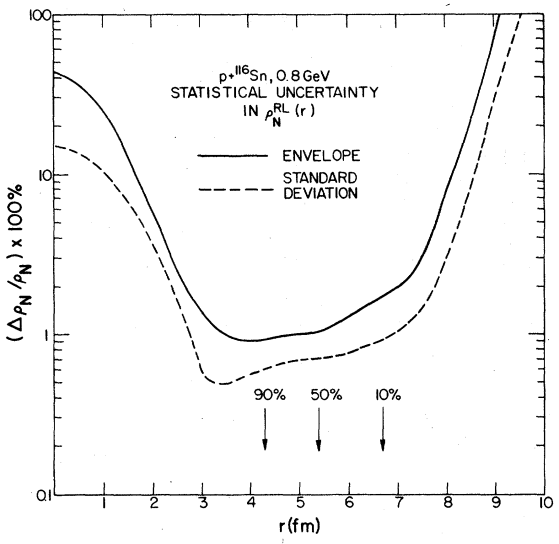

FIG. 10. Shown is the uncertainty in the RL neutron density for ^{116}Sn as a function of radial position. The solid curve results from the envelope in Fig. 6, while the dashed curve indicates the standard deviation of the numerous trial densities (see text). Effects on the deduced neutron density due to the various systematic errors (Table III) are not included here.

A comparison of the error envelopes of Figs. 4–8 with that from an analysis[10] of 1 GeV $p+^{40}$Ca data illustrates this statement. The envelope in Ref. 10 is about five times wider at the surface than those of Figs. 4–8. The statistical errors of the HRS data are typically 1–2%,[30] while for the data[4] analyzed in Ref. 10 statistical errors are 5–10%. The narrower envelope width obtained here cannot be accounted for by the somewhat higher momentum transfer considered in this analysis compared to that in Ref. 10.[58] Rather, it is due almost entirely to the higher statistical quality of the HRS data.

The nuclear interior is not as well probed as is the surface region because the RL potential is strongly absorptive at medium energies through the assumed dominant quasi-elastic absorption mechanism,[34,64] and the incident proton waves are gradually damped out within the nuclear interior. Estimating the mean free path as $d\sim(\bar{\rho}\sigma_T)^{-1}$, where $\bar{\rho}\sim 0.17$ nucleons/fm^3, one finds $d\sim 1.4$ fm for 800 MeV protons while $d\sim 0.3$ fm for 180 MeV pions. Hence, pion scattering at the (3,3) resonance would exhibit even less sensitivity to the nuclear interior than ~1 GeV protons.

Defining the kth moment of the neutron density as[10]

$$\langle r^k\rangle^{1/k} \equiv [(1/N)\int_0^\infty r^k \rho_n(r) 4\pi r^2 dr]^{1/k}, \qquad (10)$$

the moments for k ranging from -2 to 6 were computed from the random densities for each nucleus, and the mean and standard deviation for each moment were determined. Shown in Fig. 11 is the result for the ^{116}Sn RL point-neutron density; the total bandwidth plotted is 2 standard deviations. The best-determined moments for ^{116}Sn are $k=1$, 2, and 3. The range of best-determined moments increases as a function of A, so that the range $k=0-2$ is best determined for ^{58}Ni, while the range $k=2-6$ is best determined for ^{208}Pb. Hence, for all cases, the rms radius is an appropriate and well-determined parameter for comparison with findings of other experiments, and with predictions of Hartree-Fock theories, as done in Table II.

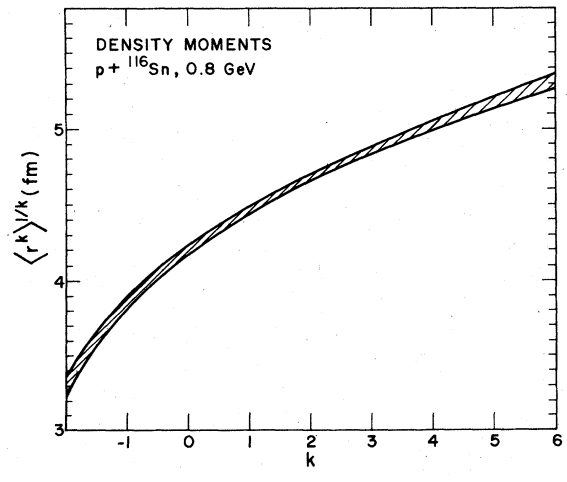

FIG. 11. Uncertainties in the various moments of the RL neutron density for ^{116}Sn. Notice that the moments for $1\leq k\leq 3$ are determined best.

D. Uncertainty in the RL neutron density due to systematic errors

A detailed investigation of the effect of systematic sources of error on the deduced neutron rms radii was also made. Considered were, (1) the experimental error in the absolute normalization and scattering angle of the proton-nucleus data,[30] (2) the uncertainty in the incident proton beam energy,[30] (3) the experimental error in the point-proton densities determined from analysis of electron scattering data,[2,58] (4) uncertainties in the parameters of the spin-dependent proton-nucleon scattering amplitudes,[45-56] and (5) the omission in the analysis of Pauli and short range dynamical correlations.[33,35]

The procedure adopted to determine the error in the deduced neutron rms radii due to 1–4 above

TABLE III. Summary of errors in $\langle r_n^2\rangle^{1/2}$ in fm. All errors are ± values.

Error Source	Magnitude	Nucleus ^{58}Ni	^{90}Zr	^{116}Sn	^{124}Sn	^{208}Pb
Normalization	±10%	0.019	0.017	0.017	0.017	0.018
$\Delta\theta_{c.m.}$	±0.03°	0.019	0.021	0.025	0.024	0.028
$\Delta\rho_p(r)$	≃±0.01 fm	0.010	0.018	0.005	0.005	0.007
ΔT_{lab}	±2 MeV	0.017	0.019	0.020	0.019	0.022
$\Delta\sigma_{pp}$	±0.5 mb	0.005	0.005	0.005	0.005	0.005
$\Delta\sigma_{pn}$	±0.22 mb	0.002	0.002	0.002	0.002	0.003
ΔB_{pp}	±0.005 fm^2	0.007	0.005	0.004	0.004	0.003
ΔB_{pn}	±0.022 fm^2	0.023	0.020	0.018	0.018	0.015
$\Delta\alpha_{pp}$	±10%[a]	0.001	0.001	0.001	0.001	0.001
$\Delta\alpha_{pn}$	±10%[a]	0.002	0.002	0.002	0.002	0.002
$\Delta(\bar\theta_p, \bar\alpha_{sp}, \bar B_{sp})$[a]		0.019	0.022	0.024	0.025	0.029
Statistical and mod. dep.[a]		0.016	0.015	0.015	0.012	0.022
Correlation (Pauli)[a]		0.025	0.021	0.019	0.019	0.018
TOTAL		0.074	0.072	0.069	0.068	0.075

[a] See text for explanation.

was to individually alter each parameter and recover the original $|\chi|^2$ by variation of the neutron densities. Several initial neutron densities were used as starting points in each search to insure that the statistical and model-dependent errors were not incorporated into any of the systematic errors. The error in $\langle r_n^2\rangle^{1/2}$ due to the omission of target nucleon-nucleon correlations was estimated from the predicted changes in the overall magnitude and slope of the cross sections when such correlations are included in the analysis.[33,35]

Second-order contributions not explicitly included were the center-of-mass correlation,[28,35] multiple-charge-exchange,[35] double spin-flip,[54,65] possible nucleon intermediate excited states,[65,66] projectile-target antisymmetrization,[67] and Fermi motion averaging.[68,69] These effects are much smaller than that due to the Pauli correlation. Third-order terms are also negligibly small.[35,70] Nonlocality effects should also be carefully considered for completeness, but such effects are generally believed to be quite small for proton scattering at intermediate energies.[71,72]

Table III summarizes the contributions to the uncertainties in $\langle r_n^2\rangle^{1/2}$ due to the systematic errors considered. A few of the entries deserve further comment. The uncertainty in the point-proton density varies according to the results of analyses[2] of electron scattering data. The uncertainty in B_{pj} was fixed by the range of slopes permitted by the proton-nucleon elastic angular distribution data,[46-49] assuming that only the two amplitudes in Eq. (1) contribute. Clearly, any statement of the values of the nucleon-nucleon amplitudes is tentative, pending a full determination of all five nucleon-nucleon amplitudes.[43] The uncertainty in α_{pj} is larger than ±10% if one considers only what is known from nucleon-nucleon scattering.[51-55] However, because the peak-to-valley ratios of the proton-nucleus angular distributions are very sensitive to $\bar\alpha_p$, the experimental error in the proton-nucleus data can be used to limit the uncertainty in α_{pj} to ±10%. The problems connected with the spin-dependent parameters were discussed in Sec. II.

E. Total uncertainty in $\rho_n^{RL}(r)$ and $\langle r^2\rangle^{1/2}$

The first twelve error-elements listed in Table III are approximately independent and add incoherently. The error due to omission of nucleon-nucleon (mainly Pauli) correlations is not independent of the other errors and is added linearly to obtain the total error given in Table III in the deduced RL point-neutron density for each nucleus considered.

It will be noticed that the total uncertainty determined here, of ±0.07 fm out of 3.5 to 5.5 fm, is significantly larger than the uncertainty often quoted in previous analyses of 1 GeV proton-nucleus scattering data,[3-12] namely ±0.03 to ±0.05 fm. It appears to the authors of this paper that these smaller errors quoted in the literature take into account only statistical error and model-dependence,[10] or alternately, uncertainty in the nucleon-nucleon scattering amplitudes,[8] but fail to include all the sources of systematic error which have been considered here. It is interesting that inclusion of Pauli correlations, particularly for the heavier nuclei, *could* reduce the overall uncertainty to ±0.05 fm, the same level that would be obtained if one eliminated the first four sources of error in Table III together with the statistical

and model-dependent error. Note also that without the spin-orbit potential, an error of ±0.03 fm would have to be added *linearly*, giving a total uncertainty in the neutron rms radius of ±0.1 fm.

A total uncertainty in $\rho_n^{RL}(r)$ due to all the effects discussed so far (statistics and finite momentum transfer of the data, systematics and Pauli correlations) was estimated for each nucleus as discussed below. For each nucleus a model density [Eq. (3)] was found which had $\langle r_n^2\rangle^{1/2}$ and $\langle r_n^4\rangle^{1/4}$ different from the density given in Table I by the total uncertainty due to the first 11 systematic errors given in Table III (the errors in the fourth moment, $\langle r_n^4\rangle^{1/4}$, are not tabulated in Table III). The second and fourth moments were used since the model densities of Table I are essentially characterized by two parameters a radius and a diffuseness. The difference between this density and that given in Table I was then interpreted as the error in $\rho_n^{RL}(r)$ due to systematic errors. In a similar way, model densities were found whose second and fourth moments were different from those of Table I by the uncertainty due to Pauli correlations, and the differences between these densities and those given in Table I were interpreted as the errors in $\rho_n^{RL}(r)$ due to the omission of Pauli correlations. The total uncertainty in $\rho_n^{RL}(r)$ was then estimated by, (1) adding incoherently the uncertainty in $\rho_n^{RL}(r)$ discussed above for the systematic errors and the standard deviations of the error envelopes shown in Figs. 4–8, and (2) adding linearly to this result the error in $\rho_n^{RL}(r)$ due to omission of Pauli correlations.

The total uncertainty found as discussed above is typically 8% to 16% at the origin, 4% at 0.9 $\rho_n^{RL}(0)$, 6% at 0.5 $\rho_n^{RL}(0)$, 16% at 0.1 $\rho_n^{RL}(0)$, and 100% at $r \sim 2\langle r_n^2\rangle^{1/2}$. Within these limits, the neutron densities predicted by the DME calculations agree well for the five cases studied with the deduced RL neutron densities at the nuclear surface. It also emerges from the analysis that the statistical error in the angular distribution data leads to a limitation of knowledge of $\rho_n^{RL}(r)$ in the nuclear interior, while the systematic errors lead to a limitation of knowledge of $\rho_n^{RL}(r)$ at the nuclear surface.

As seen in Table II, there is particularly good agreement between the DME predictions and the results of the model-independent analysis for the quantity $\Delta r_{np} = \langle r_n^2\rangle^{1/2} - \langle r_p^2\rangle^{1/2}$. When neutron rms radius differences are determined for isotopes, most systematic errors cancel, leaving only the uncertainty in the proton density and the statistical and model-dependent error. This results in an error of ±0.02 fm for the rms radius difference for the neutron distributions of ^{116,124}Sn. This underscores the general impression that comparisons between members of isotopic sequences offer a rather harsh test of Hartree-Fock predictions.

F. Total uncertainty in the imaginary part of the optical potential

On the basis of the microscopic theory of the nucleon-nucleus optical model potential,[27,28] one can argue that the least ambiguous quantity which is constructed in the analysis is the imaginary part of the optical potential, since it is this quantity which is most immediately determined by reproducing the nucleon-nucleus scattering data. Clearly, a number of further assumptions are involved in any analysis claiming to deduce reasonably unambiguous information concerning the matter density of a selected target nucleus. The sources of error which affect the determination of the imaginary part of the optical potential itself are the uncertainty in the absolute normalization and scattering angle of the experimental data, the uncertainty in the incident beam energy, the uncertainty in the real and spin-orbit terms of the optical potential, and the statistical and model-dependent uncertainties. Using the SOG technique discussed earlier the total uncertainty allowed in the imaginary part of the proton-nucleus optical potential was determined for $p+^{116}$Sn at 0.8 GeV. The results are presented in Fig. 12.

In comparing Fig. 12 to Figs. 4–8, it is important to note two important differences between the nature of the error band of the imaginary part of the optical potential and that of the RL neutron density. First, the half-width of the band shown in Fig. 12 is equal to the incoherent sum of the *standard deviations* resulting from all the sources of error listed in the previous paragraph. On the other hand, in Figs. 4–8, the *total envelope* of all trial densities which fit the available data, based on its statistical error and on model-dependence

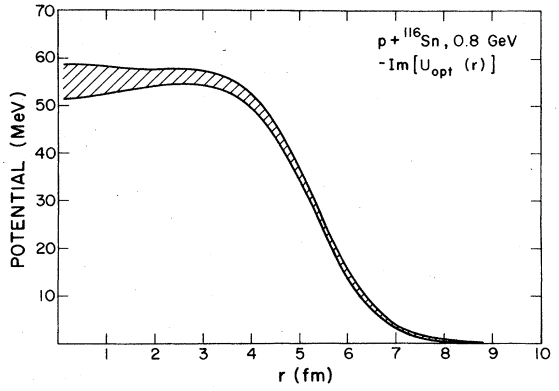

FIG. 12. Total uncertainty in the central imaginary part of the $p+^{116}$Sn optical potential at 0.8 GeV (see text).

alone, is shown. Second, the volume integral of the imaginary part of the optical potential is allowed to vary, whereas the volume integral of the RL neutron density is fixed. It is clear that the imaginary part of the optical potential is rather well determined. These findings are readily comparable to purely phenomenological analyses of medium-energy proton-nucleus elastic scattering data.[29,73]

IV. CONCLUSIONS

By means of the error analysis presented here, the usefulness of polarized medium-energy protons as probes of the neutron matter density distribution of heavy nuclei has been demonstrated. The uncertainty of the deduced neutron density has been thoroughly and quantitatively examined. Comparison of these results to those obtained, for instance, via ^{4}He elastic scattering[13-15] leaves little doubt as to which probe is the most sensitive to the distribution of nucleons in nuclei.

The approach presented here is based on a specific microscopic theory of the proton-nucleus optical potential[27,28] and although this approach is widely used and accepted, with the appearance of high quality data[5,30] it is becoming increasingly important to test the accuracy and reliability of the theory itself. A number of tests are possible. For instance, once the two-nucleon scattering amplitudes have been more accurately determined, absolute predictions of proton-nucleus analyzing powers for an $N=Z$, doubly closed-shell nucleus (for example, ^{40}Ca) could be made. These would pose a rather stringent test for the KMT theory, since the predicted analyzing powers are relatively insensitive to the uncertainty in the neutron density, and it is known that for such nuclei the neutron density is not greatly different from the known proton density.

Accurate determination of the ratio of the real to the imaginary part of the forward, spin-independent nucleon-nucleon scattering amplitude over a range of incident energies, and comparison with the proton-nucleus elastic scattering data over the same energy range, has previously also been shown to make possible a severe test of the details of the KMT approach, and to provide an indication of the precise energy range in which the approach is most applicable.[69,74,75] Also a comparison of the predicted energy dependence of the proton-nucleus total reaction cross section with the experimental results is another important test.[74]

Obtaining consistent deduced neutron densities for a range of nuclei from data covering a number of incident energies, say 200 to 2000 MeV, can provide yet another criterion for a successful theory of nucleon-nucleus elastic scattering.

Eventually, error analyses comparable or superior to those presented here should be incorporated into the presentation of results obtained with protons, ^{4}He and pions, as well as related information from total cross sections,[15,16] Coulomb energies,[20] and other techniques used to measure the neutron matter densities of nuclei. This would greatly facilitate comparisons between alternate methods and if done properly would provide definitive information as to the best method available for studying nuclear matter densities. Such comparisons will ultimately provide the most severe test of analyses such as that presented here.

Clearly, we are a long way from being able to draw conclusions concerning the validity of the KMT approach. From the quality of the fits to experimental data obtained here and elsewhere[3-12,30-33] and the good agreement with theoretical expectations,[23-26] one would not expect very serious problems to show up at 0.8 to 1.0 GeV. However, analyses at 0.6 GeV may be another story entirely.[76]

In conclusion, we, as well as others[11,12,35] have shown that the proton elastic scattering results so far obtained at 0.8 and 1.0 GeV, even when analyzed with rather different approaches to reaction theory, are in essential agreement. At least for now, immediate improvements in this type of analysis can be made by reducing the experimental systematic errors, and by carefully including higher-order corrections known to be important, such as Pauli correlations.

The authors wish to acknowledge many useful discussions with, and suggestions from, Dr. James L. Friar. This work was supported in part by the U. S. Department of Energy and the Robert A. Welch Foundation.

Note added in proof. Recent second order KMT calculations by one of us (L.R.) do not indicate any angular shifts at back angles and as a result these corrections offer no improvement in the fit beyond 20°.

[1] J. L. Friar and J. W. Negele, in *Advances in Nuclear Physics*, edited by M. Baranger and E. Vogt (Plenum, New York, 1975), Vol. 8, p. 219.
[2] C. W. de Jager, H. de Vries, and C. de Vries, At. Data Nucl. Data Tables 14, 479 (1974).
[3] G. D. Alkhazov *et al.*, Phys. Lett. 67B, 402 (1977).
[4] G. D. Alkhazov *et al.*, Nucl. Phys. A274, 443 (1976).
[5] G. S. Blanpied *et al.*, Phys. Rev. Lett. 39, 1447 (1977).
[6] I. Ahmad, Nucl. Phys. A247, 418 (1975).
[7] G. D. Alkhazov *et al.*, Phys. Lett. 57B, 47 (1975); Re-

port No. LINP-244, Leningrad, 1976 (unpublished).
[8]A. Chaumeaux, V. Layly, and R. Schaeffer, Phys. Lett. 72B, 33 (1977).
[9]L. Ray, Ph.D. thesis, University of Texas at Austin, 1977 (unpublished).
[10]I. Brissaud and M. K. Brussel, Phys. Rev. C 15, 452 (1977).
[11]G. K. Varma and L. Zamick, Phys. Rev. C 16, 308 (1977).
[12]G. K. Varma and L. Zamick (unpublished).
[13]I. Brissaud and M. K. Brussel, J. Phys. G 3, 481 (1977).
[14]E. Friedman and C. J. Batty, Phys. Rev. C 16, 1425 (1977).
[15]B. Tatischeff, I. Brissaud, and L. Bimbot, Phys. Rev. C 5, 234 (1972).
[16]G. Dugan, S. Childress, L. M. Lederman, L. E. Price, and T. Sanford, Phys. Rev. C 8, 909 (1973), and references therein.
[17]J. Hüfner, Phys. Rep. 21C, 1 (1975), and references therein.
[18]S. Iversen *et al.*, Phys. Rev. Lett. 40, 17 (1978).
[19]W. Hirt, Nucl. Phys. B9, 447 (1969).
[20]J. A. Nolen, Jr. and J. P. Schiffer, Phys. Lett. 29B, 396 (1969).
[21]H. O. Meyer, Phys. Rev. C 17, 1116 (1978).
[22]C. J. Batty and G. W. Greenlees, Nucl. Phys. A133, 673 (1969).
[23]J. W. Negele, Phys. Rev. C 1, 1260 (1970).
[24]J. W. Negele, Phys. Rev. C 9, 1054 (1974).
[25]D. Vautherin and D. M. Brink, Phys. Rev. C 5, 626 (1972).
[26]J. W. Negele and D. Vautherin, Phys. Rev. C 5, 1472 (1972), and private communication.
[27]A. K. Kerman, H. McManus, and R. M. Thaler, Ann. Phys. (N.Y.) 8, 551 (1959).
[28]H. Feshbach, A. Gal, and J. Hüfner, Ann. Phys. (N.Y.) 66, 20 (1971).
[29]R. L. Mercer, L. G. Arnold, and B. C. Clark, Phys. Lett. 73B, 9 (1978).
[30]G. W. Hoffmann, *et al.*, Phys. Rev. Lett. 40, 1256 (1978).
[31]L. Ray, G. W. Hoffmann, G. S. Blanpied, W. R. Coker, and R. P. Liljestrand, Phys. Rev. C (to be published).
[32]G. W. Hoffmann *et al.*, Phys. Lett. 76B, 383 (1978).
[33]E. Boridy and H. Feshbach, Ann. Phys. (N.Y.) 109, 468 (1977).
[34]J. Saudinos and C. Wilkin, Ann. Rev. Nucl. Sci. 24, p. 341 (1974).
[35]D. R. Harrington and G. K. Varma, unpublished.
[36]G. D. Alkhazov *et al.*, Phys. Lett. 70B, 20 (1977).
[37]G. D. Alkhazov *et al.*, Sov. Acad. Sci., 26, 715 (1977).
[38]W. R. Gibbs, B. F. Gibson, and G. J. Stephenson, Jr., Phys. Rev. Lett. 39, 1316 (1977).
[39]N. J. Digiacomo, A. S. Rosenthal, E. Rost, and D. A. Sparrow, Phys. Lett. 66B, 421 (1977).
[40]I. Sick, Nucl. Phys. A218, 509 (1974).
[41]J. L. Friar and J. W. Negele, Nucl. Phys. A240, 301 (1975).
[42]E. Boridy and H. Feshbach, Phys. Lett. 50B, 433 (1974).
[43]M. J. Moravcsik, *The Two-Nucleon Interaction* (Clarendon, Oxford, 1963), pp. 11–18.
[44]E. Kujawski and J. P. Vary, Phys. Rev. C 12, 1271 (1975).
[45]J. P. Auger, J. Gillespie, and R. J. Lombard, Nucl. Phys. A262, 372 (1976).
[46]J. Bystricky, F. Lehar, and Z. Janout, CEA-N-1547 (E), Saclay, 1972 (unpublished).
[47]O. Benary, L. R. Price, and G. Alexander UCRL Report No. UCRL-20000NN, 1970 (unpublished).
[48]H. B. Willard *et al.*, Phys. Rev. C 14, 1545 (1976).
[49]R. D. Carlini, Ph.D. thesis, University of New Mexico, 1977 (unpublished).
[50]T. J. Devlin *et al.*, Phys. Rev. D 8, 136 (1973).
[51]A. A. Vorobyov *et al.*, Phys. Lett. 41B, 639 (1972).
[52]O. V. Dumbrais, Sov. J. Nucl. Phys. 13, 626 (1971).
[53]G. Igo, in *High Energy Physics and Nuclear Structure*, edited by D. E. Nagle *et al.*, (American Institute of Physics, New York, 1975), p. 70.
[54]W. Grein and P. Kroll (unpublished).
[55]A. A. Carter and D. V. Bugg, Phys. Lett. 20, 203 (1966).
[56]P. R. Bevington *et al.*, Phys. Rev. Lett. 41, 384 (1978).
[57]M. L. Marshak *et al.*, Phys. Rev. C 18, 331 (1978).
[58]B. Frois *et al.*, Phys. Rev. Lett. 38, 152 (1977).
[59]W. R. Coker, L. Ray, and G. W. Hoffmann, Phys. Lett. 64B, 403 (1976).
[60]W. Bertozzi, J. Friar, J. Heisenberg, and J. W. Negele, Phys. Lett. 41B, 408 (1972).
[61]J. Heisenberg *et al.*, Phys. Rev. Lett. 23, 1402 (1969).
[62]J. R. Ficenec, L. A. Fajardo, W. P. Trower, and I. Sick, Phys. Lett. 42B, 213 (1972).
[63]G. W. Hoffmann *et al.*, to be published.
[64]D. M. Corley *et al.*, Nucl. Phys. A184, 437 (1972).
[65]S. J. Wallace and D. A. Sparrow, private communication.
[66]S. J. Wallace and Y. Alexander, Phys. Rev. Lett. 38, 1269 (1977).
[67]R. R. Scheerbaum, Phys. Rev. C 7, 2166 (1973).
[68]S. J. Wallace, Phys. Rev. C 12, 179 (1975).
[69]L. Ray and W. R. Coker, Phys. Rev. C 16, 340 (1977).
[70]J. J. Ullo and H. Feshbach, Ann. Phys. (N.Y.) 82, 156 (1974).
[71]F. Perey and B. Buck, Nucl. Phys. 32, 353 (1962).
[72]N. Azziz, Nucl. Phys. A147, 401 (1970).
[73]B. C. Clark, R. L. Mercer, D. G. Ravenhall, and A. M. Saperstein, Phys. Rev. C 7, 466 (1973).
[74]P. Schwaller, B. Favier, D. F. Measday, M. Pepin, P. U. Renberg, and C. Serre, CERN Report No. CERN 72-13, 1972 (unpublished); and D. F. Measday, private communication.
[75]R. C. Barrett and D. F. Jackson, *Nuclear Sizes and Structure* (Clarendon, Oxford, 1977), p. 246.
[76]G. Bruge, private communication.